

INVESTIGATION OF THE CARBONACEOUS MATTER IN ULTRACARBONACEOUS AND FINE GRAINED ANTARCTIC MICROMETEORITES. J. Rojas¹, C. M. O'D. Alexander¹, L. R. Nittler², J. Wang¹, J. Duprat³, C. Engrand⁴, E. Dartois⁵. ¹Earth and Planets Laboratory, Carnegie Institution of Washington, 5241 Broad Branch Road NW, Washington, DC 20015, USA (vrojas10@carnegiescience.edu); ²School of Earth and Space Exploration, Arizona State University, 781 Terrace Mall, Tempe, AZ 85287, USA; ³IMPMC, CNRS, MNHN, Sorbonne Univ., 75005 Paris, France; ⁴Univ. Paris-Saclay, CNRS, IJCLab, 91405 Orsay, France; ⁵Univ. Paris-Saclay, CNRS, ISMO, 91405 Orsay, France.

Introduction: Organic matter (OM) is the main C-bearing phase in primitive interplanetary samples such as meteorites and micrometeorites (MMs). Yet, the abundance of OM in these objects varies over orders of magnitude, from ~0.05 – 4 wt.% in some carbonaceous chondrites [1, 2] to ~60 wt.% in ultra-carbonaceous Antarctic micrometeorites (UCAMMs) [3-5], suggesting different formation and/or evolutionary histories. The isotopic compositions of the light elements H, C, and N can help to clarify the links between the different OMs.

The extreme C concentrations in UCAMMs, along with their high N/C ratios, suggest that they formed in specific environments that were depleted in minerals and rich in N [3, 6, 7]. Such conditions point towards a formation through the irradiation of N- and C-rich ices in the outer solar system [8-10]. Still, the H, C and N isotopic signatures of some UCAMMs echo the ones of interplanetary dust particles (IDPs) [11] and CR chondrites [1, 12, 13] formed in different environments.

To clarify the similarities and differences between the OM in UCAMMs and in other MMs and IDPs, we measure and compare the isotopic compositions and the spatial extension of carbonaceous phases in 2 UCAMMs and 1 fine-grained compact micrometeorite (FgC MM). The isotopic compositions of carbonaceous matter in fine-grained micrometeorites will provide a more complete picture of the diversity of carbonaceous phases in interplanetary samples.

Samples and Methods. We analyzed fragments from two UCAMMs (DC06-09-119 and DC06-07-18, hereafter DC06-119 and DC06-18) and one FgC MM (DC06-04-16, hereafter DC06-16) from the Concordia collection [5, 14]. The fragments of DC06-119 and DC06-16 were crushed on gold foils. The fragment of DC06-18 was pressed on a dedicated diamond cell and analyzed by IR microscopy, Raman and nanoscale infrared spectroscopy (AFM-IR) prior this study [15]. The samples were coated with a ~30 nm Au layer to ensure an optimal conductivity. The particles were analyzed with the NanoSIMS 50L instrument at the Carnegie Institution for Science. $^{16}\text{O}^-$, $^{12}\text{C}_2^-$, $^{13}\text{C}^{12}\text{C}^-$, $^{12}\text{C}^{14}\text{N}^-$, $^{12}\text{C}^{15}\text{N}^-$, $^{28}\text{Si}^-$ ion maps of the particles were acquired with a 0.5 pA primary Cs^+ ion beam. DC06-119 was mapped with a $30\times 30\ \mu\text{m}^2$ acquisition (256 \times 256 pixels, Figure 1), DC06-18 with 2 acquisitions of $17\times 17\ \mu\text{m}^2$ and $10\times 10\ \mu\text{m}^2$ (256 \times 256

pixels). Due to its larger size ($120\times 85\ \mu\text{m}$), DC06-16 was mapped with six $30\times 30\ \mu\text{m}^2$ (512 \times 512 pixels, Figure 1) acquisitions. The instrumental mass fractionations (IMFs) for $^{15}\text{N}/^{14}\text{N}$ and $^{13}\text{C}/^{12}\text{C}$ were monitored during the session using the natural anthracite DonH8, a type III kerogen, and the IOM of GRO 95502. Data were processed with the L'IMAGE software (L. Nittler) and the Matplotlib package for Python. Masks were applied to the ion images based on the C_2^- count rate to isolate carbonaceous phases in the particles. The $^{15}\text{N}/^{14}\text{N}$ and $^{13}\text{C}/^{12}\text{C}$ isotopic ratios are reported with the δ -notation as deviations from the standard values $(^{15}\text{N}/^{14}\text{N})_{\text{AIR}}$ and $(^{13}\text{C}/^{12}\text{C})_{\text{VPDB}}$.

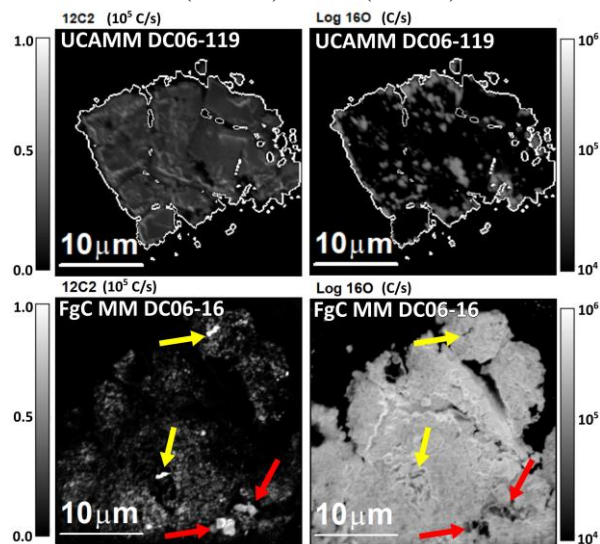


Figure 1. Top row: $^{12}\text{C}_2^-$ (left) and $\text{Log } ^{16}\text{O}^-$ (right) intensity maps of UCAMM DC06-119. The white contours indicate the edge of the particle. Bottom row: $^{12}\text{C}_2^-$ (left) and $\text{Log } ^{16}\text{O}^-$ (right) intensity maps of one of the six zones of FgC DC06-16 measured by NanoSIMS. Carbonaceous grains in DC06-16 are indicated with red arrows (high $^{12}\text{C}^{14}\text{N}^-$ emission) and yellow arrows (low $^{12}\text{C}^{14}\text{N}^-$ emission).

Results and discussion. UCAMMs DC06-119 and DC06-18. The 2 UCAMMs are characterized by their high C abundance (see surface ratios in Figure 2). Carbonaceous and O-rich mineral phases are identified with the C_2^- and $^{16}\text{O}^-$ ion images, respectively, in Figure 1 (top row), showing that C-rich phases occur as extended area, several tens of microns large. The isotopic compositions of DC06-119 and DC06-18 were

derived for 1.4- μm (DC06-18) and 3.3- μm -diameter (DC06-119) hexagonal regions of interest (ROI) tiled across the particles, resulting in a distribution of $\delta^{15}\text{N}$ and $\delta^{13}\text{C}$ values for each particle weighted by the effective surface of each ROI (red and orange bars in Figure 2). The bulk $\delta^{15}\text{N}$ and $\delta^{13}\text{C}$ of the particles are derived from the mean values of the ROIs' distributions and the heterogeneity of the samples is indicated by the standard deviation (1σ) of the distributions. DC06-119 and DC06-18 have comparable $\delta^{15}\text{N}$ and $\delta^{13}\text{C}$: $\delta^{15}\text{N}_{\text{DC06-119}} = -36 \pm 30 \text{ ‰}$, $\delta^{15}\text{N}_{\text{DC06-18}} = -55 \pm 27 \text{ ‰}$, $\delta^{13}\text{C}_{\text{DC06-119}} = 3 \pm 22 \text{ ‰}$ and $\delta^{13}\text{C}_{\text{DC06-18}} = 12 \pm 10 \text{ ‰}$. These low $\delta^{15}\text{N}$ confirm the values measured on other fragments of DC06-18 and are similar to previous results on UCAMMs [11]. The $\delta^{13}\text{C}$ of the two UCAMMs is close to 0 ‰, higher than the bulk $\delta^{13}\text{C}$ measured in the IOM of most carbonaceous chondrites [1] and compatible with previous measurements on DC06-119 [5]. The $\delta^{15}\text{N}$ signature of UCAMMs noticeably differs from the ones commonly reported for organic matter in carbonaceous chondrites and IDPs, underlining that UCAMMs (or at least some of them) probably formed from a specific precursor with a relatively light $\delta^{15}\text{N}$.

FgC MM DC06-16. The carbonaceous phases in DC06-16 occur in small, localized grains whereas most of the particle is made of minerals as shown by the C_2^- and $^{16}\text{O}^-$ emissions in Figure 1 (bottom row) and the surface fraction on Figure 2. Two different types of C-phases were identified in DC06-16:

- Grains with high C_2^- and CN^- intensities (a-type grains, red arrow in Figure 1). These grains (about 15), most probably organic, can be several microns in size and present a ^{13}C -depleted and ^{15}N -rich composition that can reach $\delta^{13}\text{C} \approx -150 \text{ ‰}$ and $\delta^{15}\text{N} \approx 400 \text{ ‰}$.
- Grains with high C_2^- and low CN^- intensities (b-type grains, yellow arrows in Figure 1). These C-phases are more abundant and have $\delta^{13}\text{C} \approx -30 \text{ ‰}$ and $\delta^{15}\text{N} \approx 0 - 500 \text{ ‰}$.

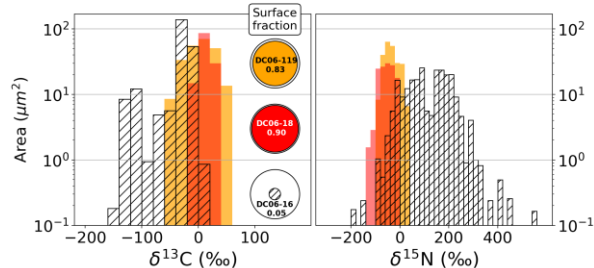


Figure 2. Histograms of the $\delta^{13}\text{C}$ (left) and $\delta^{15}\text{N}$ (right) measured in UCAMMs DC06-119 (orange), DC06-18 (red) and in the FgC MM DC06-16 (hatched). Circles on the left panel indicates the ratio of the $^{12}\text{C}_2^-$ emitting surface over the total analyzed surface of the micrometeorites, i.e., the carbonaceous surface fraction.

Noticeably, despite being separated by tens of microns, the a-type grains share very similar C and N isotopic compositions. They may have a distinct origin than the b-type grains. The ^{13}C -depletion in a-grains is comparable to values reported for the UCAMM DC06-94 [11] and for C-anomalous phases in the CO2 chondrite DOM 08006 [16] and CR3 chondrites QUE 99177 and MET 00426 [12]. However, such depletions are not commonly reported for interplanetary OM.

Figure 2 displays histograms of ROIs analyzed in DC06-119, DC06-18 and DC06-16 as a function of their $\delta^{13}\text{C}$ and $\delta^{15}\text{N}$ values. The 2 UCAMMs have bulk isotopic compositions that are distinct from the FgC MM. Although some grains in the FgC MM have a composition close to that of the 2 UCAMMs, these grains are very small in comparison to the extend areas of OM in the UCAMMs and thus, might not have formed by the same process.

Conclusions. Despite their relative rarity, UCAMMs are important carriers of organic matter that probably recorded cold volatile phases of the outer solar system. Still, their link with other extraterrestrial samples has to be clarified. New isotopic data confirm that a sub-group of UCAMMs is characterized by a negative $\delta^{15}\text{N}$ and a positive $\delta^{13}\text{C}$ compositions that are not common in other samples. Anomalous micron-scale organic grains are also reported in one FgC MM, with high ^{13}C -depletion and ^{15}N -enrichment. Similar ^{13}C -depletions have been reported in the UCAMM DC06-94 but on a much larger scale (tens of microns) [11]. A link between the OM in FgC MM and in UCAMMs may exist, however, the very different spatial distribution of the organic phases in the two objects does not make it possible to come to a firm conclusion on this point. Further investigations on the isotopic compositions of organics in UCAMMs and fine-grained MMs will be done to explore the links between C-rich phases in MMs that most probably have a cometary origin.

Acknowledgments: The work on MMs from CONCORDIA station is supported by IPEV, PNRA ANR project (COMETOR), DIM-ACAV+ (C3E) and CNES (MIAMI-H2).

References: [1] Alexander, C.M.O.D., et al., GCA, 2007. **71**(17): p. 4380-4403. [2] Alexander, C.M.O.d., et al., 2015. **50**: p. 810-833. [3] Dartois, E., et al., A&A, 2018. **609**. [4] Dobrică, E., et al., 2012. **76**: p. 68-82. [5] Duprat, J., et al., Science, 2010. **328**: p. 742-745 [6] Dartois, E., et al., Icarus, 2013. **224**: p. 243-252. [7] Yabuta, H., et al., GCA, 2017. **214**: p. 172-190. [8] Augé, B., et al., A&A, 2016. **592**: p. A99. [9] Augé, B., et al., A&A, 2019. **627**: p. A122. [10] Rojas, J., et al. in *84th An. Meet. of the Met. Soc.*, 6193. 2021. [11] Rojas, J., et al. in *LPS LII*, 1852. 2022. [12] Floss, C. and F.J. Stadermann, 2009. **697**: p. 1242. [13] Busemann, H., et al., Science, 2006. **312**(5774): p. 727-730. [14] Duprat, J., et al., Adv. Space Res., 2007. **39**: p. 605-611. [15] Mathurin, J., et al., A&A, 2019. **622**: p. A160. [16] Nittler, L.R., et al., 2018. **226**: p. 107-131.